ACS OMEGA

http://pubs.acs.org/journal/acsodf

Article

Tabletop Fabrication of High-Performance MoS_2 Field-Effect Transistors

Ungrae Cho, Seokjin Kim, Chang Yeop Shin, and Intek Song*

Cite This: *ACS Omega* 2022, 7, 21220−21224

Read Online

ACCESS | Metrics & More | Article Recommendations | Supporting Information

ABSTRACT: A simple way to prepare field-effect transistors (FETs) using MoS_2 on tabletop is presented. Conductive silver paste was applied onto chemical vapor deposition (CVD)-grown MoS_2 as Ohmic-contact electrodes. Heating the device in vacuum further enhances the performance without damage. The final performance is comparable to that of the SiO_2-backgated devices prepared by lithography and metal evaporators. The role of the silver paste and heat treatment in vacuum is investigated by device and spectroscopic analysis.

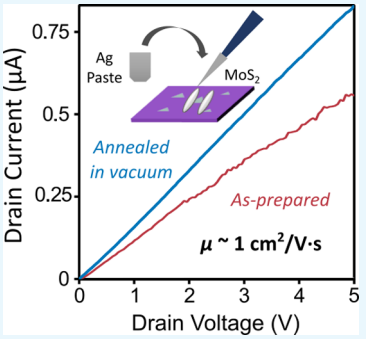

INTRODUCTION

Two-dimensional (2D) materials have been widely studied for future electronics.[1,2] They have unique properties like quantum Hall effect of graphene[3] and valley polarization of single-layered MoS_2.[4,5] The ultrathin thickness makes them useful for transparent and flexible electronics.[6] Among various 2D materials, two-dimensional MoS_2 is especially useful for electronics and related applications.[1,7−9] It has a direct band gap of 1.9 eV with strong photoluminescence and valley polarization.[4,10] And, this material has intrigued many chemists as well. Surface modification of MoS_2 can effectively modulate the electrical properties.[11] The electrical properties of MoS_2 are useful for developing chemical sensors and biosensors.[12,13] Recent advances in exfoliation[14,15] and chemical vapor deposition (CVD) techniques lower the hurdle for the preparation of high-quality specimens.[16−18]

To use the electrical properties of MoS_2, electrical devices like field-effect transistors (FETs) should be fabricated at first. However, the fabrication is not feasible for most laboratories. Typical samples obtained by chemical vapor deposition (CVD) or exfoliation techniques have random orientation and positions. So, a prototype device should be made at desired location. This is done via e-beam lithography or recently reported direct contact of nanoprobes.[19] Other methods like photolithography or shadow masking produce pre-designed devices, and the desired devices will be made only by chance. That is, a simple, economic way to prepare high-performance FETs of 2D MoS_2 would be beneficial for fundamental research.

To accomplish this goal without costly, complex processes, conductive pastes can be a viable option. Conductive pastes like Ag paste have been widely used for device fabrications of diverse materials, including two-dimensional materials.[20] However, one of the major challenges for Ag paste as electrodes is the lack of the established fabrication process and the assessment of the performance of the devices. In addition, the effect of post-fabrication treatments on conductive paste electrodes is not well studied to the best of our knowledge.

Herein, we present a simple, reproducible way to fabricate high-quality FETs within a few hours on a table. We found that this process can produce FETs, of which properties are comparable to those fabricated by shadow masking or photolithography. Also, proper heat treatment in vacuum process can substantially improve the performance of the devices.

RESULTS AND DISCUSSION

The synthesized MoS_2 is shown in Figure 1. The size of the flakes is a few tens of micrometers in diameter. The well-defined triangular shape implies that each flake consists of a single crystal. Raman spectroscopy data show that the product is single-layered MoS_2 (Figure 1c). The characteristic A_{1g} and E^1_{2g} peaks are located at ∼404 and ∼386 cm^{-1}, and the energy difference between them (∼18 cm^{-1}) corresponds to single-layered MoS_2.[21] Also, atomic force microscopy (AFM) confirmed that the thickness of the flakes is ∼1 nm, corresponding to a single layer of MoS_2[22] (Figure 1d). UV−vis spectroscopy shows the unique A and B absorption peaks of

Received: April 8, 2022
Accepted: May 30, 2022
Published: June 10, 2022

ACS Publications

© 2022 The Authors. Published by American Chemical Society

https://doi.org/10.1021/acsomega.2c02188
ACS Omega 2022, 7, 21220−21224

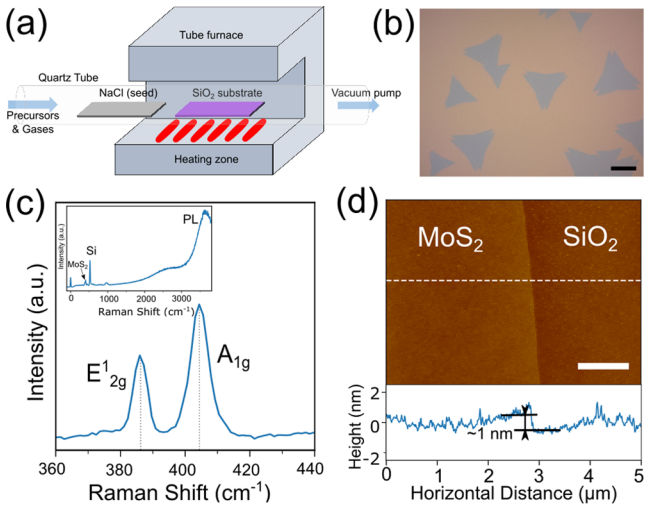

Figure 1. (a) Illustration of the CVD system. (b) Optical microscopy image of MoS_2 grown by CVD. The scale bar denotes 20 μm. (c) Raman spectrum of MoS_2 grown on the SiO_2/Si substrate. The inset shows the spectrum in a wider range. A part of photoluminescence (PL) is not shown due to the limited measurement range. (d) Atomic force microscopy image of MoS_2 on SiO_2. The graph below denotes the height profile along the white dashed line in the upper AFM image. Note that the sample was rinsed with water before the measurement to remove excess NaCl deposited during the CVD process.

MoS_2 at 650 and 610 nm, respectively (Figure S1). The wavelengths of these peaks well match with those of single-layered MoS_2; they are related to the number of layers in MoS_2 due to quantum confinement effect.[9] Similar properties are observed from filmic MoS_2 grown by the same CVD with modified growth conditions.

MoS_2-FETs were fabricated using silver paste (Figure 2). Since the size of the MoS_2 flakes is small, fabricating the devices using an optical microscope and applying partially dried paste can facilitate the process (refer to Materials and Methods for details). Note that a fresh SiO_2/Si substrate is recommended for the back-gate oxide. This is because direct fabrication onto the very substrate used in CVD often results in high leakage current. This can be attributed to the damage of the thin oxide layer during the high temperature synthesis process.[23] Therefore, MoS_2 was transferred onto a fresh substrate before fabricating devices (refer to Methods and Materials for the details). The electrical measurement of the FET in air before heating in vacuum is shown in Figure 3a,c. The $I_{DS}-V_{DS}$ curve (or the output curve) is linear near 0 V, suggesting the Ohmic contact. The $I_{DS}-V_{GS}$ curve (or the transfer curve) shows n-type doping of the device with a high on-off ratio (~4000). The estimated charge carrier mobility with W/L ~1 in this case is ~0.5 $cm^2/V\cdot s$. The devices were then heated in a vacuum oven at 200 °C in vacuum (<5 Pa) for 2 h. After heating the same device in vacuum, the characteristics of the device were further improved (Figure 3b,d). The noise of the curves was significantly reduced despite the same measurement condition. The conductivity, the on-off ratio (>7000), and the charge carrier mobility (~1.09 $cm^2/V\cdot s$) were all increased. In addition, no apparent change in hysteresis was found as a result of the thermal treatment in vacuum. To check the reproducibility of the device fabrication process, we obtained statistics of the performance by characterizing multiple devices. The average mobility before annealing was 6.31×10^{-1} $cm^2/V\cdot s$, and it was then increased to 1.02 $cm^2/V\cdot s$ after being annealed in vacuum with reduced noise (Figure S2). And, this value of charge carrier mobility is comparable to other SiO_2-backgated devices measured in air.[8,24] This protocol can be applied to filmic MoS_2 as well. And heat treatment in vacuum is still effective for filmic MoS_2 devices (Figure S3). This shows that this technique can be applied not only to single-crystalline flakes but also to polycrystalline films.

Applying silver paint and heating it in vacuum is, therefore, a very efficient way to prepare high-quality devices without complex machines. The high efficiency of this process is at first attributed to silver. Ag is known as an efficient electrode material for MoS_2.[25] Ag has a work function of 4.26 eV, which is comparable to Ti (4.33 eV). But unlike Ti or other metals, Ag does not react with MoS_2, forming a stable junction.[25] Indeed, the Ohmic contact of the electrode is well reproduced, and does not change upon heating in vacuum. This is contrary to Ti/Au electrode prepared by metal evaporators; their contacts are often changed by thermal annealing or e-beam irradiation.[26,27] The chemical inertness of Ag makes the paint an optimal choice for handling the device in air as well.

Regarding the thermal treatment in vacuum, it did not trigger any visual change in the optical microscopy images (Figure S4). To investigate in depth, MoS_2 grown on a quartz substrate, with the same growth parameters as the SiO_2/Si substrates, was analyzed by UV−vis spectroscopy (Figure 4). Pre-annealed samples have four bands in the spectra. Two major bands at 1.89 eV (blue) and 2.03 eV (red) are attributed to A and B absorption bands of pristine MoS_2.[4,9] The other minor bands at 1.83 eV (green) and 1.99 eV (yellow) are not found from pristine MoS_2 and had lower energy. After being annealed in vacuum, the spectrum resembles pristine MoS_2; the minor bands disappeared while the major bands were retained. Thermal treatment also changed the PL spectrum; the peak was shifted from 1.84 to 1.88 eV (Figure S5).

Two possible explanations to the phenomenon are (i) healing of defects and (ii) removal of surface contaminants. The former

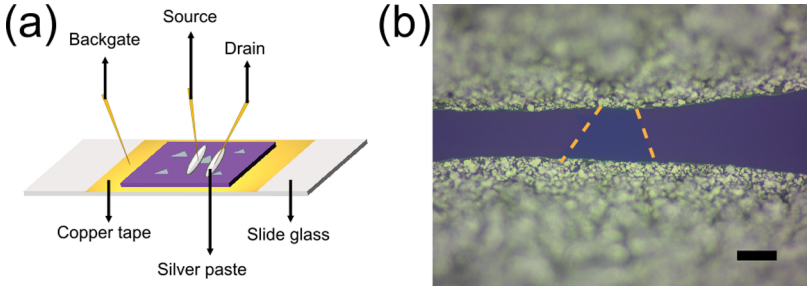

Figure 2. (a) Scheme of a device with silver paint as an electrode. (b) Optical microscopy image of a fabricated device. The scale bar denotes 20 μm. The orange dashed line presents the outer boundary of the MoS_2 flake.

https://doi.org/10.1021/acsomega.2c02188
ACS Omega 2022, 7, 21220−21224

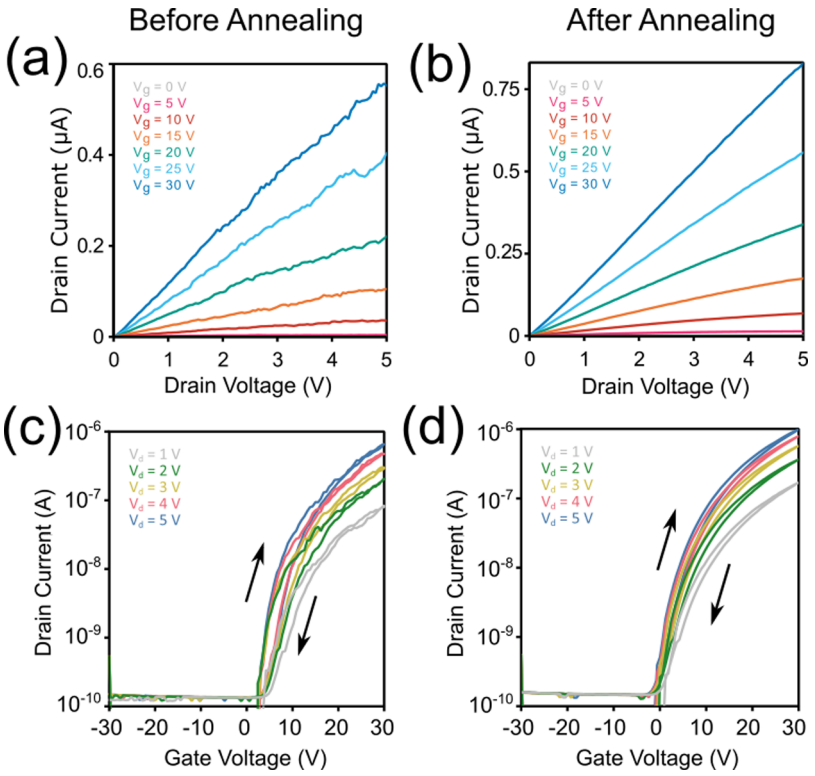

Figure 3. (a–d) Output (a, b) and transfer (c, d) curves of the MoS_2 FET with silver paste electrodes, measured in air at room temperature. The transfer curves were measured by sweeping the gate voltage. (a) and (c) are the characteristics of the device before annealing, and (b) and (d) are those of the same device after annealing. The different colors of the graphs show the changing gate (a, b) and drain voltage (c, d). The arrows in (c) and (d) show the direction of measurement of each hysteresis loop; the upper half of the loop was measured by increasing the gate voltage and the lower half of the loop was measured by decreasing it.

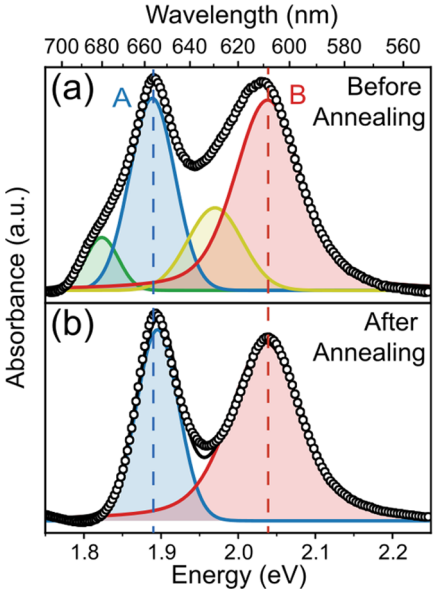

Figure 4. UV–vis absorption spectrum of MoS_2 (a) before and (b) after annealing. The baseline of the raw data was corrected for peak fitting. Note that (a) is an excerpt from Figure S1. The circles show the absorption spectrum data, and the solid lines show the envelop (black) and fitting peaks (colored). The vertical dashed lines show the energy of the main absorption peaks of MoS_2: blue for A and red for B absorption bands.

is unlikely in this case. There was no supply of precursors during the annealing process, and the temperature is far below the evaporation temperature of MoS_2.[28] Also, n-type conductivity, often attributed to S vacancies, still remained after the in-vacuo annealing process (Figure 3d). In contrast, the latter can account for the result. Surface adsorbates, whether physisorbed or chemisorbed, alter the band structure of MoS_2.[29] These adsorbates can be generated during their synthesis, device fabrication, or even during their storing in air. Heating under vacuum can effectively remove surface contaminants that have relatively low volatility. Indeed, evacuation without heating was not able to improve the device performances (Figure S6), but the effect of heat treatment in vacuum persisted after exposure to air (Figure 3b,d). This shows that surface contaminants generate impurity levels between the conduction band and the valence band. And, this results in the evolution of absorption peaks of lower energy as well as the degradation of the performance. In addition, the blue-shift of the PL implies that possible adsorbates would be water or oxygen, which can form Mo–O bonds.[30] The formation of Mo–O bonds can alter the PL profiles, and annealing MoS_2 in air by removing the Mo–O bonds causes a blue-shift of the PL peaks. This further implies that heating in vacuum effectively removes these adsorbates without altering the MoS_2 or MoS_2-Ag electrode interface.

CONCLUSIONS

In conclusion, silver paste electrodes can produce MoS_2 FETs with performance comparable to those prepared by lithography and metal evaporation. And, the simple post-fabrication annealing process can significantly improve the performances of the devices. The reason for the success of this protocol is (i) the use of silver paint, which does not require annealing, and (ii)

https://doi.org/10.1021/acsomega.2c02188
ACS Omega 2022, 7, 21220–21224

heat treatment in vacuum, which removes redundant band structures for better performance of the devices. We believe that our findings would lower the hurdle for developing various applications of FETs in many fields.

MATERIALS AND METHODS

MoS_2 was prepared by chemical vapor deposition after the recommendation of Kang et al.[17] and Song et al.[31] (Figure 1a). A SiO_2 (300 nm)/Si substrate (p-type, Namkang Hi-tech) or a quartz substrate was loaded into a one-inch quartz tube. For the growth of large flakes, 300 sccm of Ar and 5 sccm of H_2 were then supplied into the tube with vacuum pumping near 1 Torr. The tube was then heated up to 650 °C using a tube furnace. When the temperature reached the target temperature, $Mo(CO)_6$ (Acros organics, 98%) and 0.3 sccm of $(C_2H_5)_2S$ (Alfa Aesar, 96%) were supplied into the tube. The amount of $Mo(CO)_6$ was controlled by a metering valve (SS−SS1-VH, Swagelok). In this experiment, the metering valve was adjusted to 10 in the vernier scale. After 18 h, the supply of the precursors was stopped, and the sample was cooled down to room temperature while the carrier gases were continuously supplied. As the temperature reached room temperature, the sample was taken out of the tube for further analysis. For the growth of filmic products, the overall process is the same as the flake synthesis, except for minor adjustment in the growth parameters. For example, no NaCl was used, and the metering valve was adjusted to 20 in the vernier scale. Also, the reaction duration was extended to 24 h.

An optical microscope (Eclipse LV150NL, Nikon) was used to check the morphology of the MoS_2 flakes. The quality of the synthesized MoS_2 was analyzed by the Raman spectrometer (WITec alpha300R with a Nd:YAG laser (wavelength: 532 nm)), atomic force microscope (Nanoscope IIIa, Digital Instrument Inc.), and UV−vis spectrometer (S-3100, Scinco). Before the AFM measurement, the sample was rinsed with water to remove excess NaCl deposited during the CVD process. UV−vis spectra were analyzed by a custom-made program (Python 3.7 with NumPy and SciPy package). The baseline of the spectrum was corrected by asymmetric least squares smoothing.

To transfer MoS_2 onto an fresh SiO_2/Si substrate, we referred to Suk et al.[32] to prevent the degradation of MoS_2. First, 9% PMMA (MW 350k, Sigma Aldrich) dissolved in anisole (99.0%, Samchun) was spin-coated onto the as-received MoS_2/SiO_2 (1000 rpm for 10 s followed by 3000 rpm for 30 s). Then, the sample was floated onto 1 M KOH (aq) to detach the SiO_2/Si substrate. After being detached, the sample was floated on fresh deionized water for 1 h to remove remaining KOH, and it was repeated three times. Then, the sample was finally transferred onto a fresh SiO_2/Si substrate. After remaining water was drained, it was placed on a hotplate at 180 °C to enhance the adhesion between the MoS_2 layer and the SiO_2/Si substrate. It was then cooled down to room temperature, and the remaining PMMA was removed by immersing the sample in acetone.

To fabricate FET devices, silver paste (product no. 16040-30, Ted Pella) was used as the electrode material. A large drop of the paste was at first applied on a clean glass substrate to remove the excess solvent of the paste, methyl isobutyl ketone (MIBK). A wooden needle was used to apply the paste onto the MoS_2 flakes under an optical microscope. The prepared device was then dried in air for up to an hour to completely remove the paste at room temperature.

For heat treatment in vacuum, we used a vacuum oven (SH-VDO-08NG, SH Scientific). The devices were heated at 200 °C in vacuum for 2 h. The pressure inside the oven was maintained at less than 5 Pa.

The measurement of the electrical devices was done using a semiconductor analyzer (model 2636B, Keithley) and a vacuum-compatible probe station (MPS-VAC, Nextron). All measurements were carried out at room temperature.

ASSOCIATED CONTENT

Supporting Information

The Supporting Information is available free of charge at https://pubs.acs.org/doi/10.1021/acsomega.2c02188.

UV−vis absorption spectrum of MoS_2; statistics of charge carrier mobility before and after thermal treatment in vacuum; device characteristics of filmic MoS_2; optical microscopy image of the devices after annealing; photoluminescence shift of MoS_2 by thermal treatment in vacuum; and the FET device performance measured in vacuum (PDF)

AUTHOR INFORMATION

Corresponding Author

Intek Song − *Department of Applied Chemistry, Andong National University (ANU), Andong 36729 Gyeongbuk, Republic of Korea;* orcid.org/0000-0001-5213-6696; Email: songintek@anu.ac.kr

Authors

Ungrae Cho − *Department of Applied Chemistry, Andong National University (ANU), Andong 36729 Gyeongbuk, Republic of Korea*

Seokjin Kim − *Department of Applied Chemistry, Andong National University (ANU), Andong 36729 Gyeongbuk, Republic of Korea*

Chang Yeop Shin − *Department of Applied Chemistry, Andong National University (ANU), Andong 36729 Gyeongbuk, Republic of Korea*

Complete contact information is available at: https://pubs.acs.org/10.1021/acsomega.2c02188

Author Contributions

U.C. and I.S. conceived the experiments. U.C. and S.K. carried out the experiment. U.C., C.Y.S., and I.S. performed FET device fabrication and analysis. U.C., C.Y.S., and I.S. performed AFM measurement, preparation, and analysis. All authors contributed to data analysis and writing of this manuscript.

Funding

This research was supported by the National Research Foundation of Korea (NRF) grant funded by the Korea government (MSIT) (No. 2021R1F1A1050074).

Notes

The authors declare no competing financial interest.

REFERENCES

(1) Chhowalla, M.; Shin, H. S.; Eda, G.; Li, L.-J.; Loh, K. P.; Zhang, H. The Chemistry of Two-Dimensional Layered Transition Metal Dichalcogenide Nanosheets. *Nat. Chem.* **2013**, *5*, 263−275.

(2) Nevalaita, J.; Koskinen, P. Atlas for the Properties of Elemental Two-Dimensional Metals. *Phys. Rev. B* **2018**, *97*, No. 035411.

(3) Zhang, Y.; Tan, Y.-W.; Stormer, H. L.; Kim, P. Experimental Observation of the Quantum Hall Effect and Berry's Phase in Graphene. *Nature* **2005**, *438*, 201−204.

(4) Mak, K. F.; He, K.; Shan, J.; Heinz, T. F. Control of Valley Polarization in Monolayer MoS2 by Optical Helicity. *Nat. Nanotechnol.* **2012**, *7*, 494−498.
(5) Zeng, H.; Dai, J.; Yao, W.; Xiao, D.; Cui, X. Valley Polarization in MoS2 Monolayers by Optical Pumping. *Nat. Nanotechnol.* **2012**, *7*, 490−493.
(6) Kim, K. S.; Zhao, Y.; Jang, H.; Lee, S. Y.; Kim, J. M.; Kim, K. S.; Ahn, J.-H.; Kim, P.; Choi, J.-Y.; Hong, B. H. Large-Scale Pattern Growth of Graphene Films for Stretchable Transparent Electrodes. *Nature* **2009**, *457*, 706−710.
(7) Song, I.; Park, C.; Choi, H. C. Synthesis and Properties of Molybdenum Disulphide: From Bulk to Atomic Layers. *RSC Adv.* **2015**, *5*, 7495−7514.
(8) Radisavljevic, B.; Radenovic, A.; Brivio, J.; Giacometti, V.; Kis, A. Single-Layer MoS2 Transistors. *Nat. Nanotechnol.* **2011**, *6*, 147−150.
(9) Mak, K. F.; Lee, C.; Hone, J.; Shan, J.; Heinz, T. F. Atomically Thin ${\mathrm{MoS}}_{2}$: A New Direct-Gap Semiconductor. *Phys. Rev. Lett.* **2010**, *105*, No. 136805.
(10) Splendiani, A.; Sun, L.; Zhang, Y.; Li, T.; Kim, J.; Chim, C.-Y.; Galli, G.; Wang, F. Emerging Photoluminescence in Monolayer MoS_2. *Nano Lett.* **2010**, *10*, 1271−1275.
(11) Sim, D. M.; Kim, M.; Yim, S.; Choi, M.-J.; Choi, J.; Yoo, S.; Jung, Y. S. Controlled Doping of Vacancy-Containing Few-Layer MoS_2 *via* Highly Stable Thiol-Based Molecular Chemisorption. *ACS Nano* **2015**, *9*, 12115−12123.
(12) Sarkar, D.; Liu, W.; Xie, X.; Anselmo, A. C.; Mitragotri, S.; Banerjee, K. MoS_2 Field-Effect Transistor for Next-Generation Label-Free Biosensors. *ACS Nano* **2014**, *8*, 3992−4003.
(13) Perkins, F. K.; Friedman, A. L.; Cobas, E.; Campbell, P. M.; Jernigan, G. G.; Jonker, B. T. Chemical Vapor Sensing with Monolayer MoS_2. *Nano Lett.* **2013**, *13*, 668−673.
(14) Zhou, K.-G.; Mao, N.-N.; Wang, H.-X.; Peng, Y.; Zhang, H.-L. A Mixed-Solvent Strategy for Efficient Exfoliation of Inorganic Graphene Analogues. *Angew. Chem., Int. Ed.* **2011**, *50*, 10839−10842.
(15) Novoselov, K. S.; Jiang, D.; Schedin, F.; Booth, T. J.; Khotkevich, V. V.; Morozov, S. V.; Geim, A. K. Two-Dimensional Atomic Crystals. *Proc. Natl. Acad. Sci.* **2005**, *102*, 10451−10453.
(16) Song, I.; Park, C.; Hong, M.; Baik, J.; Shin, H.-J.; Choi, H. C. Patternable Large-Scale Molybdenium Disulfide Atomic Layers Grown by Gold-Assisted Chemical Vapor Deposition. *Angew. Chem., Int. Ed.* **2014**, *53*, 1266−1269.
(17) Kang, K.; Xie, S.; Huang, L.; Han, Y.; Huang, P. Y.; Mak, K. F.; Kim, C.-J.; Muller, D.; Park, J. High-Mobility Three-Atom-Thick Semiconducting Films with Wafer-Scale Homogeneity. *Nature* **2015**, *520*, 656−660.
(18) Lee, Y.-H.; Zhang, X.-Q.; Zhang, W.; Chang, M.-T.; Lin, C.-T.; Chang, K.-D.; Yu, Y.-C.; Wang, J. T.-W.; Chang, C.-S.; Li, L.-J.; Lin, T.-W. Synthesis of Large-Area MoS2 Atomic Layers with Chemical Vapor Deposition. *Adv. Mater.* **2012**, *24*, 2320−2325.
(19) Iemmo, L.; Urban, F.; Giubileo, F.; Passacantando, M.; Di Bartolomeo, A. Nanotip Contacts for Electric Transport and Field Emission Characterization of Ultrathin MoS2 Flakes. *Nanomaterials* **2020**, *10*, 106.
(20) Seo, J.-W. T.; Zhu, J.; Sangwan, V. K.; Secor, E. B.; Wallace, S. G.; Hersam, M. C. Fully Inkjet-Printed, Mechanically Flexible MoS_2 Nanosheet Photodetectors. *ACS Appl. Mater. Interfaces* **2019**, *11*, 5675−5681.
(21) Lee, C.; Yan, H.; Brus, L. E.; Heinz, T. F.; Hone, J.; Ryu, S. Anomalous Lattice Vibrations of Single- and Few-Layer MoS_2. *ACS Nano* **2010**, *4*, 2695−2700.
(22) Song, J.-G.; Ryu, G. H.; Lee, S. J.; Sim, S.; Lee, C. W.; Choi, T.; Jung, H.; Kim, Y.; Lee, Z.; Myoung, J.-M.; Dussarrat, C.; Lansalot-Matras, C.; Park, J.; Choi, H.; Kim, H. Controllable Synthesis of Molybdenum Tungsten Disulfide Alloy for Vertically Composition-Controlled Multilayer. *Nat. Commun.* **2015**, *6*, No. 7817.
(23) Song, I.; Park, Y.; Cho, H.; Choi, H. C. Transfer-Free, Large-Scale Growth of High-Quality Graphene on Insulating Substrate by Physical Contact of Copper Foil. *Angew. Chem., Int. Ed.* **2018**, *57*, 15374−15378.
(24) Huo, N.; Yang, Y.; Wu, Y.-N.; Zhang, X.-G.; Pantelides, S. T.; Konstantatos, G. High Carrier Mobility in Monolayer CVD-Grown MoS_2 through Phonon Suppression. *Nanoscale* **2018**, *10*, 15071−15077.
(25) Schauble, K.; Zakhidov, D.; Yalon, E.; Deshmukh, S.; Grady, R. W.; Cooley, K. A.; McClellan, C. J.; Vaziri, S.; Passarello, D.; Mohney, S. E.; Toney, M. F.; Sood, A. K.; Salleo, A.; Pop, E. Uncovering the Effects of Metal Contacts on Monolayer MoS_2. *ACS Nano* **2020**, *14*, 14798−14808.
(26) Pelella, A.; Kharsah, O.; Grillo, A.; Urban, F.; Passacantando, M.; Giubileo, F.; Iemmo, L.; Sleziona, S.; Pollmann, E.; Madauß, L.; Schleberger, M.; Di Bartolomeo, A. Electron Irradiation of Metal Contacts in Monolayer MoS_2 Field-Effect Transistors. *ACS Appl. Mater. Interfaces* **2020**, *12*, 40532−40540.
(27) Liu, W.; Kang, J.; Cao, W.; Sarkar, D.; Khatami, Y.; Jena, D.; Banerjee, K.High-Performance Few-Layer-MoS2 Field-Effect-Transistor with Record Low Contact-Resistance. In *2013 IEEE International Electron Devices Meeting*; IEEE: Washington, DC, 2013; pp 19.4.1−19.4.4, DOI: 10.1109/IEDM.2013.6724660.
(28) Wu, S.; Huang, C.; Aivazian, G.; Ross, J. S.; Cobden, D. H.; Xu, X. Vapor−Solid Growth of High Optical Quality MoS_2 Monolayers with Near-Unity Valley Polarization. *ACS Nano* **2013**, *7*, 2768−2772.
(29) Yue, Q.; Shao, Z.; Chang, S.; Li, J. Adsorption of Gas Molecules on Monolayer MoS2 and Effect of Applied Electric Field. *Nanoscale Res. Lett.* **2013**, *8*, No. 425.
(30) Wei, X.; Yu, Z.; Hu, F.; Cheng, Y.; Yu, L.; Wang, X.; Xiao, M.; Wang, J.; Wang, X.; Shi, Y. Mo-O Bond Doping and Related-Defect Assisted Enhancement of Photoluminescence in Monolayer MoS_2. *AIP Adv.* **2014**, *4*, No. 123004.
(31) Song, I.; Choi, H. C. Revealing the Role of Gold in the Growth of Two-Dimensional Molybdenum Disulfide by Surface Alloy Formation. *Chem. - Eur. J.* **2019**, *25*, 2337−2344.
(32) Suk, J. W.; Kitt, A.; Magnuson, C. W.; Hao, Y.; Ahmed, S.; An, J.; Swan, A. K.; Goldberg, B. B.; Ruoff, R. S. Transfer of CVD-Grown Monolayer Graphene onto Arbitrary Substrates. *ACS Nano* **2011**, *5*, 6916−6924.

https://doi.org/10.1021/acsomega.2c02188
ACS Omega 2022, 7, 21220−21224